

Cover Page



Universiteit Leiden



The handle <http://hdl.handle.net/1887/21063> holds various files of this Leiden University dissertation.

Author: Ewing, Mark McConnell

Title: Post-interventional atherosclerotic vascular remodeling : preclinical investigation into immune-modulatory therapies

Issue Date: 2013-05-23

Chapter 6

Optimizing natural occurring IgM antibodies for therapeutic use: inflammatory vascular disease treatment with anti-phosphorylcholine IgG

M.M. Ewing^{1,2,3}, J.C. Karper^{2,3}, M. Nordzell⁴, S.A.P. Karabina⁵, R. Atout⁵, D. Sexton⁶, H. Lettesjö⁷, M.R. de Vries^{2,3}, I. Dahlbom⁴, O. Camber⁴, J. Frostegård⁸, J. Kuiper⁹, E. Ninio⁵, J.W. Jukema^{1,3}, K. Pettersson⁴, P.H.A. Quax^{2,3}

1 Dept. of Cardiology, Leiden University Medical Center (LUMC), Leiden, The Netherlands

2 Dept. of Surgery, LUMC, Leiden, The Netherlands

3 Eindhoven Laboratory for Experimental Vascular Medicine, LUMC, Leiden, The Netherlands

4 Athera Biotechnologies, Stockholm, Sweden

5 INSERM UMRS937, Université Pierre et Marie Curie UPMC-Paris and Faculté de Médecine Pierre et Marie Curie, Paris, France

6 Dyax Corporation, Cambridge, MA, USA

7 Dept. of Women's and Children's Health, Uppsala University Hospital, Uppsala, Sweden

8 Dept. of Medicine, Karolinska University Hospital Huddinge and Karolinska Institutet, Stockholm, Sweden

9 Division of Biopharmaceutics, LACDR, Leiden, The Netherlands

Submitted for publication

Abstract

Background Phosphorylcholine (PC) is an important pro-inflammatory damage associated molecular pattern and natural anti-PC T15 IgM antibodies are both clinical risk markers for cardiovascular diseases and prevent native atherogenesis in mice. For clinical use, however, only IgGs are suitable, but major variability exists in natural anti-PCs IgG effects.

Methods and results Chimeric anti-PC T15 IgG was developed and shown to bind locally to human atherosclerotic tissues. Following immunization of hyperlipidemic ApoE3*Leiden mice undergoing femoral arterial cuff placement to induce vascular inflammation and remodeling, 73.6% reduced atherosclerotic lesion size was observed ($p=0.0003$), with reduced expression of local ER-stress markers and MCP-1 production.

Phage display-library screening led to the development of three fully human monoclonal anti-PC IgG constructs which specifically bound PC and apoptotic cells and prevented both macrophage oxLDL-uptake and their MCP-1 expression in vitro, superiorly to natural anti-PC T15 IgM antibodies. Of these, anti-PC M99-B05 IgG was most effective in vivo by reducing inflammation and atherosclerotic lesion size with 61.4% ($p=0.014$). Germ lining and codon optimization of M99-B05 produced anti-PC X19-A05 IgG, which was as effective as M99-B05 in vivo, even in low dosages.

Conclusions Both chimeric and fully human anti-PC IgGs can prevent post-interventional atherosclerotic lesion formation by inhibiting injury-induced vascular inflammation directly and through reduced macrophage oxLDL-uptake. These could represent a novel strategy for prevention of post-interventional atherosclerotic lesion development.

Introduction

Although treatments for atherosclerosis-induced acute coronary syndromes (ACS) have improved patient outcome greatly in the last decades, there is still much room for improvement, especially for treatment modalities that target increased local vascular inflammatory burden after myocardial infarction¹. In this acute phase, cellular stress and inflammation can lead to the generation of endogenous ligands. These ligands, such as phosphorylcholine (PC), have recently been described as damage associated molecular patterns (DAMPs) that are recognized by the innate immune system². PC is the polar headgroup of the dominating membrane phospholipid phosphatidylcholine. In cellular stress and inflammation as well as during enzymatic and oxidative modification of LDL the fatty acids of phosphatidylcholine, especially the fatty acids in the sn-2 position, are metabolized. Many of these PC containing metabolites (oxPL) have powerful biological effects and are considered important mediators of vascular inflammation. A recent review summarized these effects and concluded that oxPL is a promising therapeutic target³. There are several receptors recognizing PC including proteins, scavenger receptors of phagocytic cells and natural antibodies^{2, 4}. PC recognition has been reported to stimulate a range of responses including endothelial dysfunction, apoptosis, endoplasmatic reticulum (ER)-stress and the unfolded protein response (UPR)^{5, 6}. They all lead to vascular inflammation, eventually responsible for accelerated atherosclerotic lesion formation, often requiring revascularization⁷. Interestingly, there is competition between these receptors and the prototypic natural anti-PC, the murine T15/E06 IgM, is well known to inhibit macrophage binding and uptake of oxLDL through scavenger receptors⁸.

Uptake of oxLDL by vessel wall macrophages is considered as a pro-atherogenic event⁹, while anti-PC has anti-atherosclerotic effects. Immunization leading to high anti-PC levels can prevent native atherosclerosis in mice by inhibition of oxLDL-uptake and inflammatory foam cell formation¹⁰⁻¹². Epidemiological data suggests that IgM anti-PC protects against cardiovascular disease (CVD) development, as low levels of the IgM anti-PC are associated with increased risks for CV events¹³⁻¹⁵. Additionally, ACS patients with low levels of IgM anti-PC have a worse prognosis than patients with higher levels¹⁶. The increased risk was particularly present in the semi-acute phase following ACS, during which there is an elevated systemic inflammatory activity¹⁷. Experimental data shows that the T15/E06 natural antibodies also have profound anti-inflammatory properties unrelated to foam cell formation and enhance clearance of apoptotic cells^{18, 19}. This suggests that they could also be therapeutically effective in the acute injury phase following ACS, during which there is still a high risk for secondary events.

Experimental data has principally been generated using the natural IgM anti-PC. Serum contains anti-PCs of several subclasses²⁰ and not all may be able to block vascular inflammatory processes. Hypertensive patients display an inverse correlation between the progression of carotid artery intima media thickness and IgM anti-PC titers, but not for IgG anti-PCs²¹. While T15 IgM was effective against *Streptococcus* infections in mice, there was major variability in IgG anti-PCs effects²²⁻²⁴. These results indicate that although PC is a chemically defined entity, the presentation of the PC (neo)epitope depends on the local environment and that different IgG anti-PCs may be more specific for the presentation of PC than the natural IgM anti-PC.

IgM antibodies are not suitable for therapeutic use. The aim of this work was to investigate if anti-PC in an IgG format has the potential to block vascular inflammation, and to identify a fully human monoclonal anti-PC that has therapeutic potential. We first generated an anti-PC T15 IgG chimeric antibody that prevented inflammatory vascular disease both in vitro and in vivo, providing support that anti-PC IgGs are attractive as therapeutic antibodies. We then identified multiple, fully human recombinant anti-PC IgGs by phage-display library screening. These were selected and optimized for their in vitro and in vivo anti-inflammatory and anti-atherosclerotic effects, with potential to become a new treatment modality against post-interventional vascular remodeling.

Materials and Methods

The materials and methods sections can be found in the online supplements section.

Results

Chimeric anti-PC T15 IgG binds to human atherosclerotic lesions and is effective against vascular inflammation in vivo

A chimeric anti-PC T15 IgG antibody was developed, containing the murine T15/E06 variable region and human IgG1 in the constant region, highly specific for PC. Immunohistochemical (IHC) staining with chimeric anti-PC T15 IgG showed strong and specific binding to cells within human aortic atherosclerotic lesions (fig 1a), confirmation of antibody affinity for the target tissue. Next, therapeutic effectiveness of chimeric anti-PC T15 IgG was tested in a well-established mouse model for post-interventional inflammatory vascular disease²⁵. Short term leukocyte recruitment and long-term vascular remodeling were evaluated.

Despite similar plasma total cholesterol concentrations (table 2), chimeric anti-PC T15 IgG (plasma titer 1208 ± 329 $\mu\text{g/ml}$) significantly reduced endothelial-adherence and extravasation of leukocytes (fig 1c) and macrophages (fig 1c) to the injured arterial segments 3d after injury, prior to foam cell development. Furthermore, anti-PC T15 IgG staining displayed strong and specific co-localisation with GRP78 BiP and CHOP expressing cells, suggesting specific binding of T15 IgG to PC-expressing stressed cells within atherosclerotic plaques. Treatment significantly reduced cells displaying ER-stress markers CHOP and GRP78BiP by 73.0% ($p=0.021$, fig 2b) and 54.7% ($p=0.050$, fig 2c) respectively. Together, these results indicate that anti-PC T15 IgG prevents early inflammatory responses, well before the generation of local foam cells²⁶.

Chimeric anti-PC T15 IgG is effective against vascular remodeling in vivo

Vascular remodeling was evaluated after 14d treatment (fig 3a) and revealed that despite similar plasma cholesterol levels (table 2), anti-PC T15 IgG significantly prevented intimal thickening by 76.3% ($p=0.0003$, fig 3b) and reduced intima/media ratio by 72.2% ($p=0.000$, fig 3c), luminal stenosis by 60.3% ($p=0.000$, fig IIa) and medial thickening by 20.0% ($p=0.050$, fig IIb). After 14d, the medial arterial layer displayed a less inflamed phenotype, with a higher proportion of stable SMCs (87.0%,

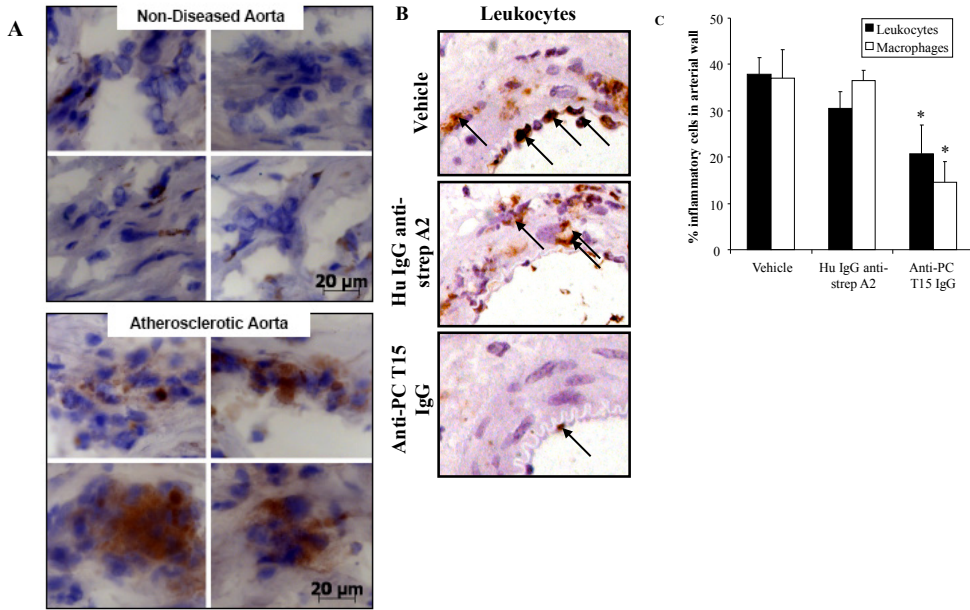


Figure 1 Representative cross-sections of (A) human non-diseased and atherosclerotic aortic tissue (chimeric anti-PC T15 IgG staining, magnification 20x) and of cuffed arteries of ApoE3*Leiden mice receiving vehicle, human anti-streptavidin or anti-PC T15 IgG (B) after 3d (CD45 staining, magnification 80x, arrows indicate leukocytes). Quantification of (C) leukocyte and macrophages (% of total cells). Results indicated as mean±SEM, n=10. * p<0.05.

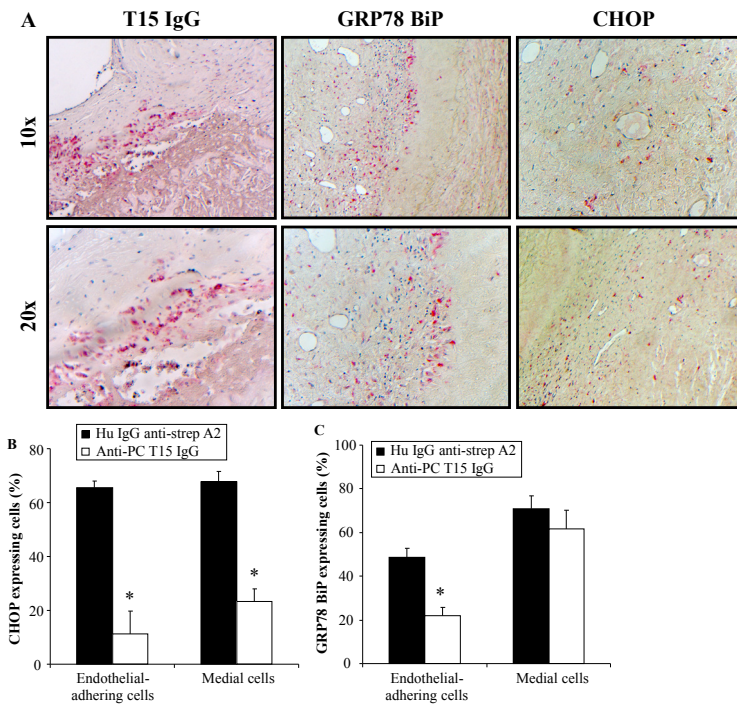
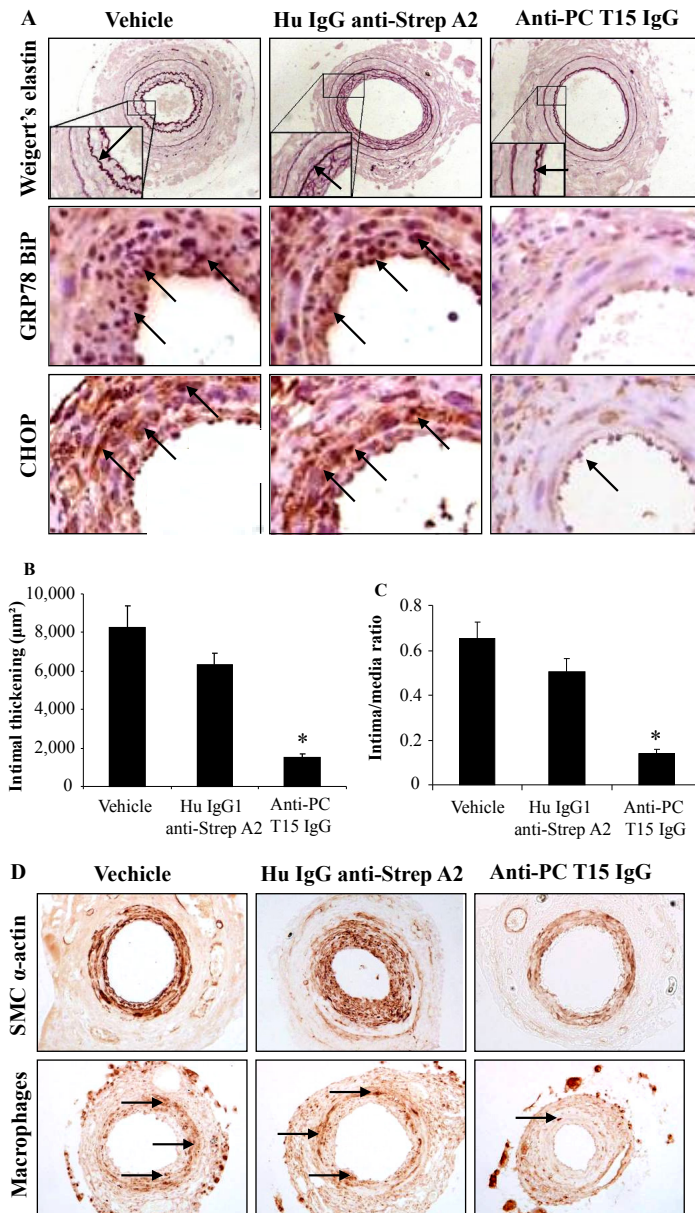


Figure 2 Representative cross-sections of (A) human atherosclerotic coronary arteries (chimeric anti-PC T15 IgG, GRP78 BiP and CHOP staining, magnification 10-20x). Quantification of cuffed arteries of ApoE3*Leiden mice receiving vehicle, human anti-streptavidin or anti-PC T15 IgG after 3d for cells expressing (B) CHOP (% of total cells) and (C) GRP78 BiP (% of total cells). Results indicated as mean±SEM, n=10. * p<0.05.

p=0.016, fig 3e) and 72.2% less macrophages (p=0.000, fig 3f). Anti-PC T15 IgG also reduced leukocyte infiltration in the intima and media by 66.0% (p=0.001, fig 3h) and 74.2% (p=0.002, fig 3i).



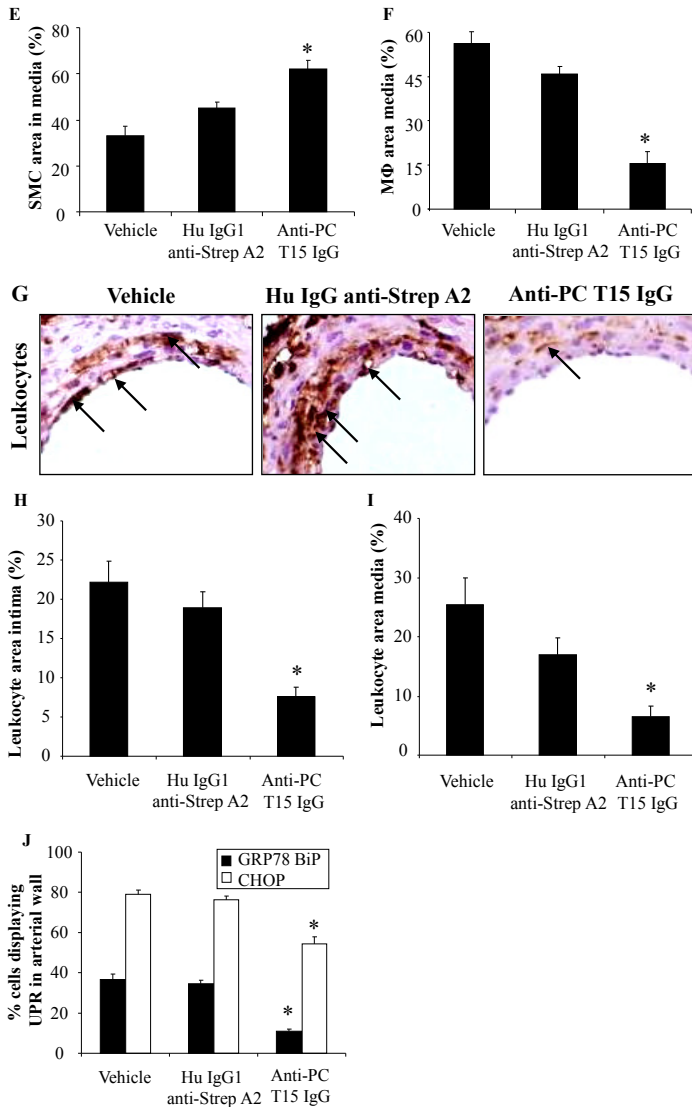


Figure 3 Representative cross-sections of cuffed arteries of ApoE3*Leiden mice receiving vehicle, human anti-streptavidin or anti-PC T15 IgG after 14d (A Weigert's elastin, GRP78 BiP and CHOP staining, D SMC- α actin and MAC3 staining; G CD45 staining; magnification 40-80x). Quantification of (B) intimal thickening (μm^2), (C) intima/media ratio, (E) SMCs in the media (% of total area), (F) macrophages in the media (% of total area), (H) leukocytes in the intima (% of total), (I) leukocytes in the media (% of total) and (J) ER-stressed cells (% of total cells). Results indicated as mean \pm SEM, n=10. * p<0.05.

Furthermore, anti-PC T15 IgG significantly reduced cells displaying ER-stress markers CHOP (absent before injury, fig 1Ic) and GRP78BiP by 31.4% (p=0.0003) and 70.4% (p=0.0003, fig 3j), demonstrating that chimeric anti-PC T15 IgG prevents the inflammatory UPR, involved in inflammatory vascular remodeling.

Unlike murine anti-PC IgM, chimeric anti-PC T15 IgG does not block oxLDL-

uptake by macrophages

Polyclonal IgM and IgG anti-PC obtained from human serum were evaluated to block the uptake of oxLDL particles by macrophages, as the murine T15/E06 IgM natural antibody is known to block this scavenger receptor-mediated uptake¹⁰. As expected, polyclonal anti-PC IgMs showed a dose-dependent (fig IIIa-b) inhibition of DiI-labelled Cu-oxLDL uptake (fig 4a), whereas polyclonal anti-PC IgGs did not (fig 4b). Previously, low concentrations of polyclonal human anti-PC IgG from serum following active immunization was shown to partly inhibit oxLDL-uptake in macrophages¹¹. Similar results were obtained with 20 $\mu\text{g}/\text{ml}$ anti-PC IgG, but not with higher concentrations (fig 4c). Cimeric anti-PC T15 IgG also did not prevent Cu-oxLDL uptake by human macrophages (fig 4d).

Unlike IgM, the Fc region of IgG1 bears a highly conserved N-glycosylation site that is essential for Fc receptor-mediated activity by macrophages and could lead to increased antibody-PC complex binding by macrophages and oxLDL-uptake. This possibility was excluded by using both a chimeric anti-PC T15 IgG4 antibody, as IgG4 antibodies are less prone to bind Fc receptors (fig 4d), as well as Fc-receptor blocking anti-CD32 and anti-CD64 antibodies (fig IIIc), through which no blocked oxLDL-uptake was observed. Although effective *in vivo*, at least partly through UPR downregulation, the transfer of the T15/E06 variable region from IgM to IgG format abolished the scavenger receptor blocking effects of chimeric anti-PC T15 IgG.

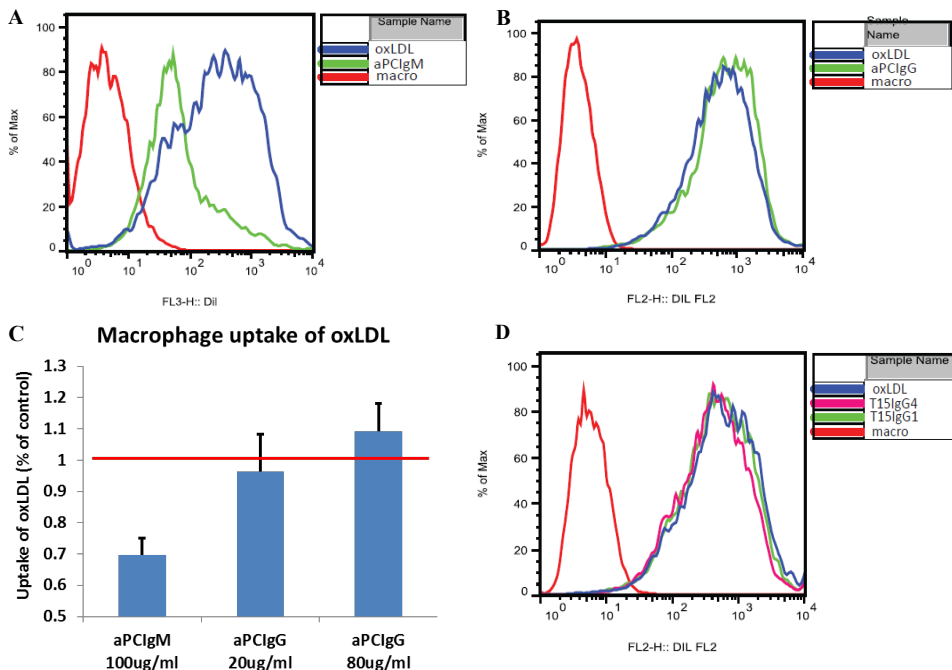


Figure 4 FACS analysis demonstrates that unlike murine anti-PC IgM (A), polyclonal anti-PC IgG does not block oxLDL-uptake by macrophages (B), in both low (20 $\mu\text{g}/\text{ml}$) and high (80 $\mu\text{g}/\text{ml}$) concentrations (C). Both IgG1 and IgG4 antibodies fail to display an inhibiting effect (D), excluding the potential enhanced Fc-receptor-regulated uptake of oxLDL.

Development of monoclonal human anti-PC IgG antibodies

Fully human, monoclonal IgG antibodies against PC were obtained by phage display by panning human Fab fragment displayed libraries²⁷ against either BSA- or ferritin-conjugated PC. Over ten thousand different phage clones were screened by ELISA, which yielded over 1500 positive hits, defined as > 3-fold stronger signal for binding to BSA- or ferritin-conjugated PC compared to streptavidin-coated controls. After DNA sequencing and recombinant reformatting to full length IgG1 51 antibodies with unique amino acid sequences were recovered. Binding specificity was assessed using a Biacore SPR assay to binding to either PC-BSA or a control BSA containing the aminophenol linker that used for the conjugation of PC to BSA, allowing selection of antibodies with likely therapeutic effectiveness, also shown by ELISA (fig 5a). Of these, 27 antibodies with highest signal for binding PC-BSA were investigated for their effects on macrophage oxLDL-uptake. Nine fully human recombinant anti-PC IgG antibodies inhibited oxLDL-uptake similarly or better than polyclonal anti-PC IgM on a weight basis (fig 5b).

These 9 monoclonal IgGs displayed approximately 1000-fold higher binding efficacy to PC than polyclonal IgG anti-PC, as measured in an ELISA (fig 5c). Antibodies M99-B05 and X9-C01, potent inhibitors of oxLDL uptake, were analysed for binding to Cu-oxidized LDL and displayed profound increased binding compared to chimeric anti-PC T15 IgG (fig 5d). The lack of effect of chimeric anti-PC T15 IgG to block oxLDL-uptake is probably explained by the poor binding to oxLDL. The high avidity of the murine IgM T15/E06 to PC compared to IgG isotype probably explains the effectiveness of the IgM isotype anti-PC¹⁸. Antibodies with high apparent affinity for PC and oxLDL were tested for binding to apoptotic Jurkat cells using FACS analysis. Only marginally increased binding to cells considered as early apoptotic (annexin A5+ PI-) compared to normal viable cells was found. Some antibodies, including M99-B05, were found to bind strongly to late apoptotic (annexin A5+ PI+) Jurkat cells (fig 5e-h), while others did not. Four selected antibodies were finally tested for their ability to block oxLDL-induced release of MCP-1 from monocytes and both M99-B05 and X9-C01 effectively blocked this release in a dose-dependent fashion with an IC₅₀ in the 1-3 nM range whilst the other tested antibodies were ineffective (fig 5i). M99-B05 displayed strong and specific binding to human atherosclerotic aortic tissue, unlike HRP streptavidin controls (fig IVa).

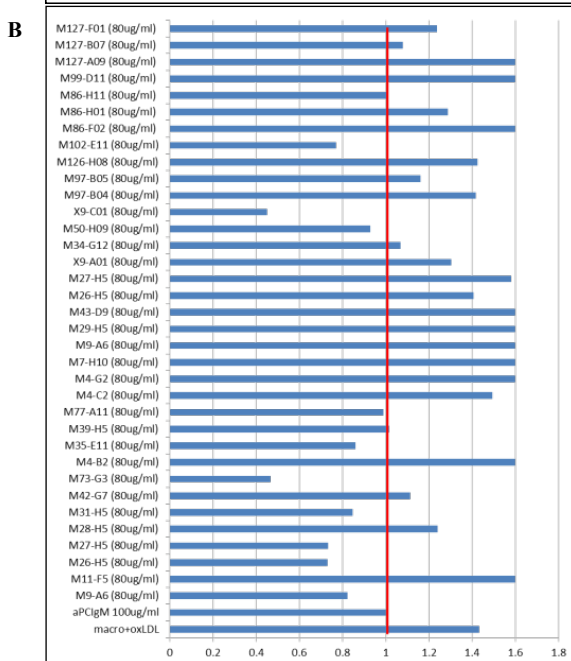
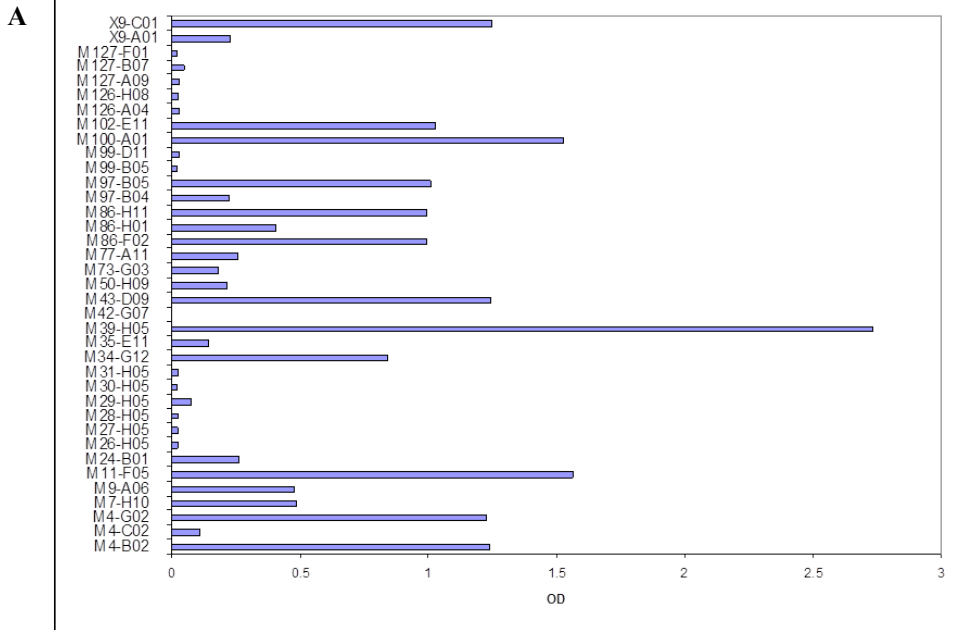
Monoclonal human anti-PC IgGs are effective against vascular inflammation in vivo

The anti-inflammatory properties of X9-C01, M73-G3 and M99-B05 were tested in vivo in the femoral artery cuff mouse model, with chimeric anti-PC T15 IgG, Hu a-strep A2 IgG and sterile water as controls (fig Va). Despite similar plasma lipid concentrations and antibody titers (tables 2, 3), 3d treatment with anti-PC M99-B05 reduced the endothelial-adherence and extravasation of leukocytes by 60.9% ($p=0.021$), macrophages by 48.9% ($p=0.006$, fig 6a) and MCP-1 expressing cells by 81.7% ($p=0.003$, fig 6c), while other antibodies were less effective.

Monoclonal human anti-PC IgG is effective against vascular remodeling in vivo

Despite similar plasma lipid concentrations and antibody titers (table 2, 3), twice weekly immunization with 10mg/kg M99-B05 significantly prevented vascular remo-

deling, with reduced intimal thickening by 61.4% ($p=0.014$, fig 6e), intima/media ratio by 58.3% ($p=0.008$, fig 6f) and outward remodeling by 35.3% ($p=0.039$, fig VIa) after 14d. Luminal stenosis was reduced by 20.7%, although not significantly ($p=0.160$, fig VIb). IHC analysis from human aortic atherosclerotic lesions revealed specific M99-B05 staining (fig 6g) in macrophage-rich areas.



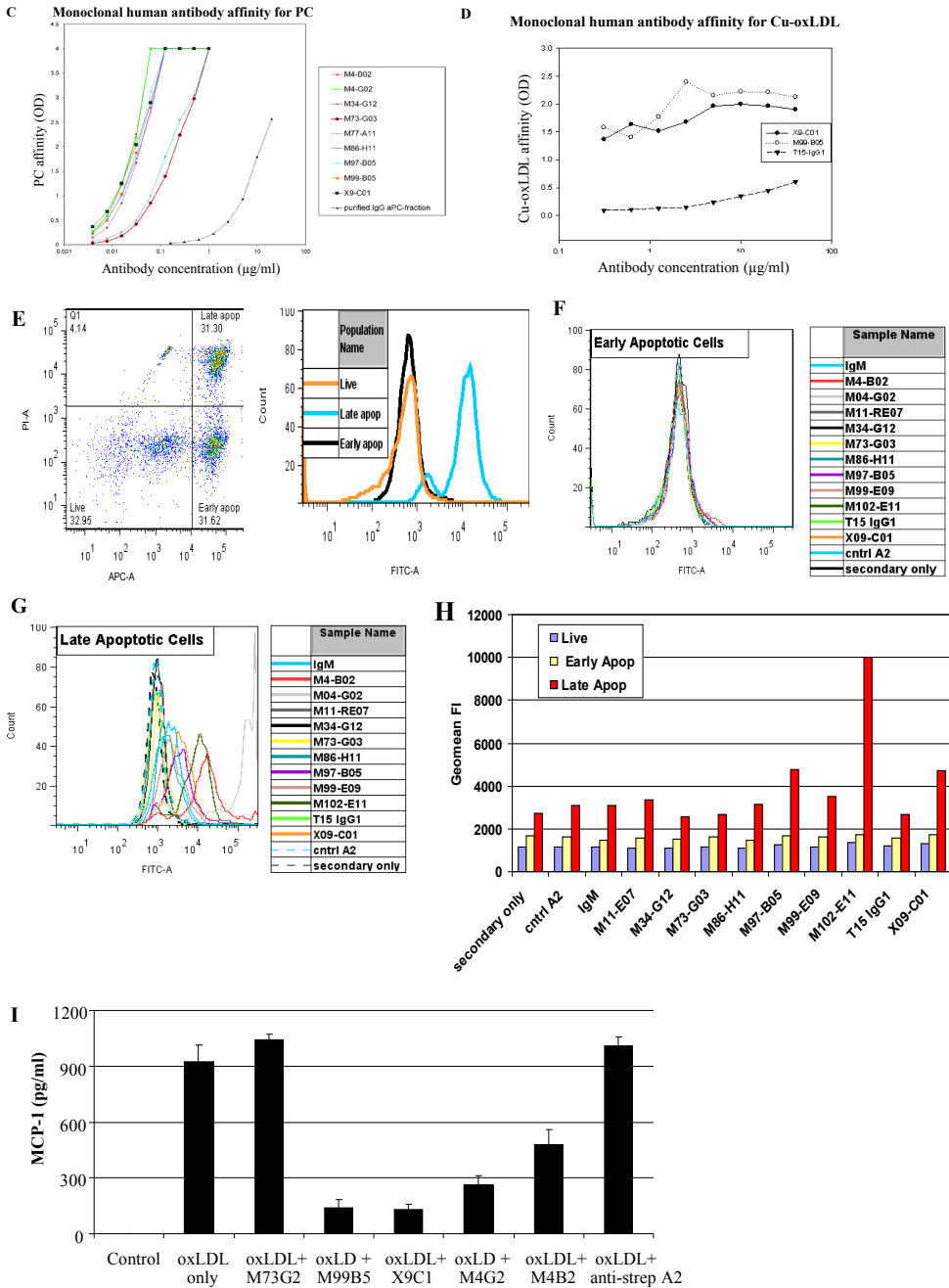


Figure 5 Antibody binding efficacy by 27 clones to BSA-PC (A), inhibitory effects on macrophage oxLDL-uptake of nine selected antibody clones compared to anti-PC IgM (B), and their affinity to PC (C) and oxLDL (D), measured through ELISA (expressed as OD). Of these, 7 antibodies had approximately 1000-fold higher affinity to PC than polyclonal IgG anti-PC. FACS analysis of dot plot showing (E) different cell populations after staurosporine inducing, including live cells (annexin A5-PI-), (F) early apoptotic cells (annexin A5+PI-) and (G) late apoptotic cells (annexin A5+PI+). (H) Mean fluorescent intensity of each cell

population. (I) MCP-1 release assay of human monocytes stimulated with oxLDL alone or in combination with antibody clones (pg/ml) with $IC_{50}=1.8 \pm 0.74$ nM for anti-PC M99B05 IgG.

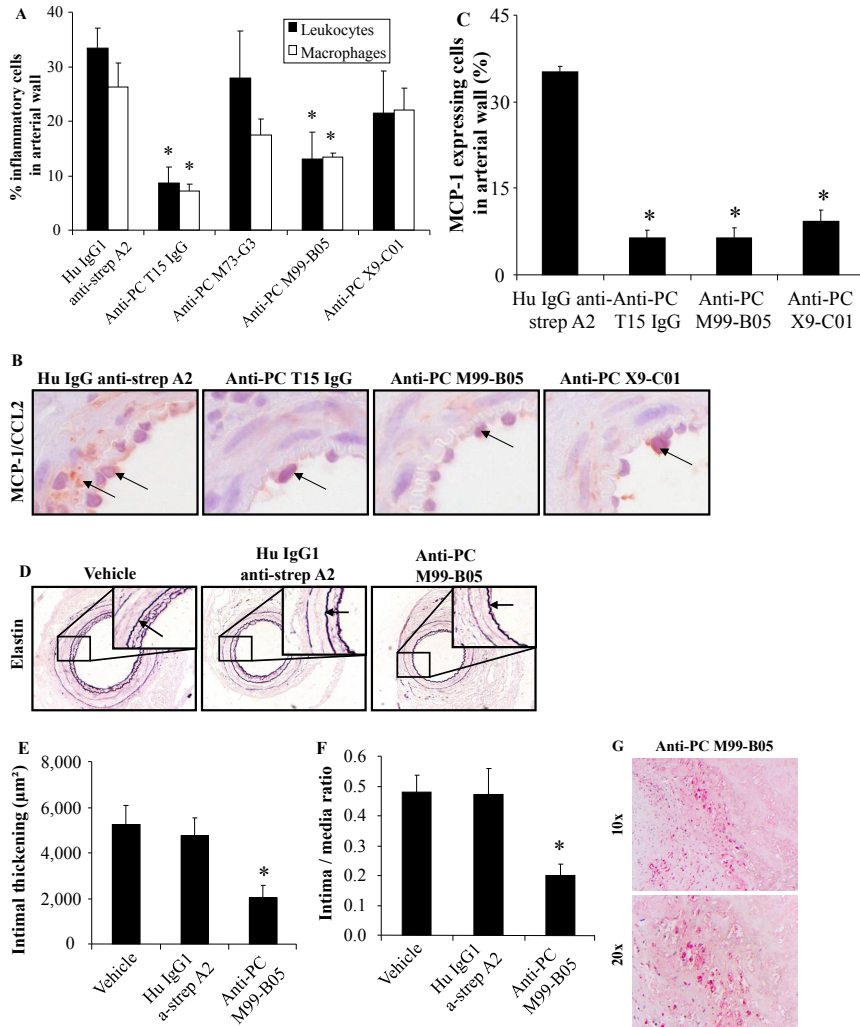


Figure 6 Representative cross-sections of cuffed arteries of ApoE3*Leiden mice receiving human anti-streptavidin, anti-PC T15, M99-B05 or X9-C01 (B) after 3d (MCP-1 staining), (D) 14d (Weigert's elastin staining) or (G) human atherosclerotic coronary artery sections (anti-PC M99-B05 staining, magnification 10-80x). Quantification of after 3d (A) leukocyte and macrophages (% of total cells), and after 14d (C) MCP-1 expressing cells (% of total cells), (E) intimal thickening (μm^2) and (F) intima/media ratio. Results indicated as mean \pm SEM, n=10. * p<0.05.

Optimization of monoclonal human anti-PC M99-B05 into X19-A05

A site-directed mutagenesis study was performed to determine which CDR regions were involved in binding PC, providing insight into the paratope of M99-B05. A 3-D model of M99-B05 was constructed (fig VIIa) together with an amino acid sequence analysis (fig VIIb, c), designed to obtain a full characterization of the antigen-antibody interaction. Western-Blot analysis showed good antibody stability in serum (fig

VII d, e). Codon optimization produced a series of M99-B05 mutants that had some replacements for potential de-amidation sites constructed. These were tested for the binding to PC (ELISA) and it was observed that some modifications of the M99-B05 antibody negatively affected binding affinity to PC (fig 7a). The mutant X19-A05 was selected as the optimal antibody, as it combines several modifications of M99-B05 while retaining good binding affinity to PC.

X19-A05 anti-PC IgG is effective in vivo in low dosages

Despite similar plasma lipid concentrations and antibody titers (tables 2, 3), 14d treatment with X19-A05 anti-PC in twice weekly 0.5, 2 and 10mg/kg dosages significantly prevented intimal thickening by 40.1% ($p=0.024$), 46.8% ($p=0.014$) and 67.6% ($p=0.000$) respectively, similarly to M99-B05, when compared to Hu a-strep A2 IgG controls (fig 7c), with 10 mg/kg 17.5% more effective ($p=0.031$) than 0.5mg/kg. Versus vehicle, 0.5, 2 and 10m/kg X19-A05 anti-PC reduced reduced the intima / media ratio by 38.9% ($p=0.042$), 39.1% ($p=0.018$) and 56.1% ($p=0.002$, fig VIII a). In conclusion, the optimized monoclonal X19-A05 anti-PC IgG antibody retained the therapeutic effectiveness of M99-B05 and forms a promising antibody clone for clinical use to prevent post-interventional vascular remodeling.

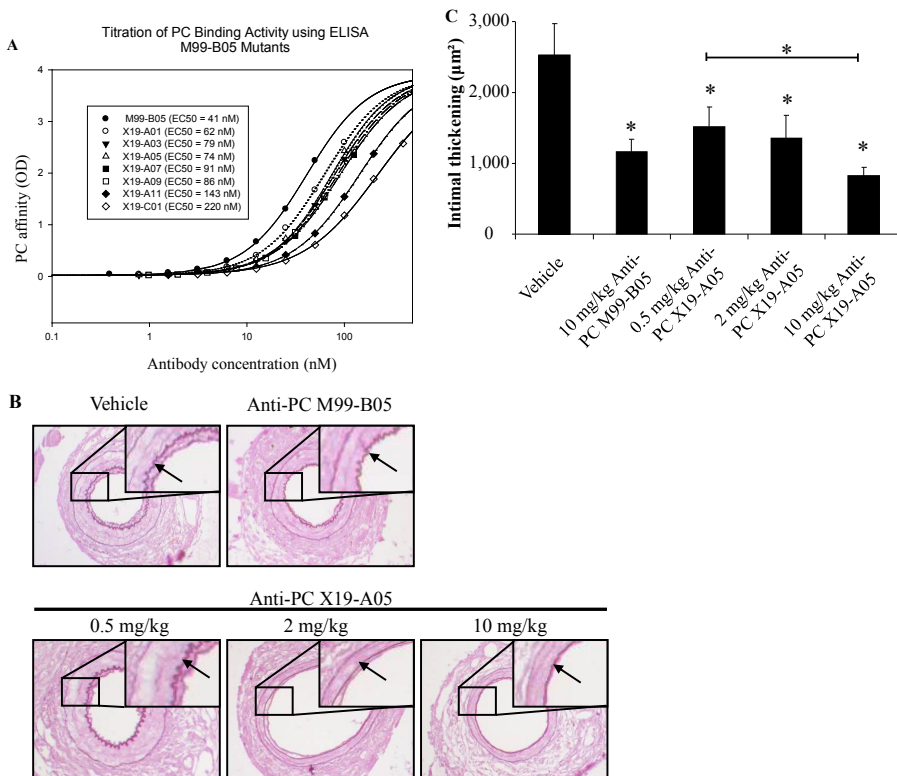


Figure 7 PC-affinity by seven M99-B05 clones, measured by ELISA (expressed as OD) (A). Representative cross-sections (B) of cuffed arteries of ApoE3*Leiden mice receiving human anti-streptavidin, M99-B05 or X19-A05 (0.5, 2, 10mg/kg) after 14d (Weigert's elastin staining, magnification 40x). Quantification of (C) intimal thickening (μm^2). Results indicated as mean \pm SEM, n=10. * $p<0.05$.

Discussion

This study demonstrates for the first time natural anti-PC IgM antibody optimization and therapeutic efficacy of a phage-library display selected monoclonal human anti-PC IgG construct against inflammatory atherosclerotic disease. Passive *in vivo* immunization with chimeric anti-PC T15 IgG prevented inflammatory arterial disease including UPR and atherosclerotic remodeling. Since natural anti-PC IgM antibodies display inhibition of oxLDL-uptake by macrophages and this function was lost by the chimeric anti-PC T15 IgG, monoclonal human anti-PC IgGs were screened for this function. These proved to be effective *in vivo* by profoundly reducing inflammation and atherosclerotic remodeling.

Research into new monoclonal recombinant antibodies is a fast-developing and expanding field and atherosclerotic-related CVDs with high incidence, prevalence and mortality rates¹ are extremely suitable for therapeutic immunization strategies. PC plays a key role as DAMP in the inflammatory reaction in both native atherosclerosis and following vascular intervention strategies. In the latter setting, it has emerged as a promising target for active immunization to prevent vascular remodeling. Until now, successful therapeutic immunization against PC has mostly been on an IgM basis in mice, whilst for clinical application, IgG-based vaccination is preferred²⁸.

Specific chimeric anti-PC T15 IgG binding was observed in human atherosclerotic lesions with distinctive co-localization with regions displaying signs ER stress (fig 1-2a), proving antibody binding to the target tissue. In hyperlipidemic mice, chimeric anti-PC T15 IgG effectively reduced leukocyte and macrophage adherence and extravasation following vascular injury (fig 1c), with notably less MCP-1 expression by adhered and infiltrated leukocytes (fig 1d), clearly showing therapeutic efficacy. Due to hypercholesterolemia, α -actin SMCs display markers of early ER-stress (fig 1Ib), whilst this progressed to advanced ER-stress and UPR following vascular injury. Defective inflammatory resolution is known lead to the progression of atherosclerotic lesions^{29,30} and by reduction of ER-stress and UPR-induced inflammation, prolonged anti-PC T15 IgG treatment led to retarded occlusive vascular remodeling (fig 3b) and a less inflammatory arterial wall phenotype (fig 3g).

Polyclonal anti-PC IgMs showed an inhibition of oxLDL-uptake by macrophages *in vitro*, whereas polyclonal anti-PC IgGs did not. Similarly, chimeric anti-PC T15 IgG also did not prevent oxLDL-uptake by macrophages *in vitro* (fig 4d), an effect unrelated to Fc receptor-mediated activity in IgG1 antibodies by macrophages, making them unsuitable for clinical use to prevent native atherosclerosis. Post-interventional vascular remodeling however does not primarily result from oxLDL-uptake, but from local cellular (ER) stress and DAMP expression, followed by leukocyte chemotaxis (e.g. through MCP-1) and inflammation. Although this concept supports the chimeric anti-PC T15 IgG effectiveness in the murine vascular injury model, vascular remodeling can be enhanced through oxLDL-uptake by infiltrated macrophages. Since these processes occur simultaneously in the human ACS setting, phage library-display selection was used to screen for monoclonal human anti-PC IgGs that have both anti-inflammatory effects and an ability to block oxLDL-uptake. Recombinant antibody libraries provide a solid basis for the discovery of antibody-based biopharmaceuticals³¹ and are an excellent source of active and well tolerated experimental therapeutics³². IgGs were selected upon their binding capability to PC and apoptotic

cells, as well as their ability to block macrophage oxLDL uptake and MCP-1 expression in vitro (fig 5g). Out of a total 10.660 phage clones, these selection criteria yielded three promising antibody clones, designated M99-B05, X9-C01 and M73-G3.

Only anti-PC M99-B05 significantly reduced leukocyte and macrophage adherence and infiltration in the injured local arterial wall segments (fig 6a), although both M99-B05 and M73-G03 reached high plasma titers, whereas X9-C01 did not. It cannot be excluded that X9-C01 could be effective in similar concentrations, although M73-G3 was clearly ineffective. Despite this, effects of prolonged anti-PC M99-B05 treatment were investigated and displayed reduced vascular thickening, proving its long-term efficacy (fig 6e). In combination with strong local binding to atherosclerotic human arterial segments (fig 6g), this makes the anti-PC M99-B05 clone a promising therapeutic antibody for clinical use.

To increase production efficacy, reduce immunogenicity and increase antibody stability in serum, codon optimization of M99-B05 anti-PC was performed. PC-affinity assays and in vivo application clearly showed preserved PC-affinity and therapeutic efficacy (fig 8b), even in low dosages (2mg/kg/twice weekly).

The limited time period (14d) of antibody exposure was used to minimize the generation of murine anti-human IgG antibodies, although their development cannot be ruled out. Furthermore, despite in vitro and in vivo therapeutic effectiveness, murine results cannot be extrapolated to the human situation automatically. Nevertheless, anti-PC X19-A05 IgG has been shown to be a promising therapeutic tool.

The present findings show that PC is a promising therapeutic target in the prevention of accelerated atherosclerosis development, suitable for passive therapeutic immunization with recombinant monoclonal antibodies. By providing direct control of the patient's immune response with restriction to a single immunogenic epitope, this immunization approach could prove to be an effective treatment modality against CVD in patients.

Reference List

1. Lloyd-Jones D, Adams R, Carnethon M, et al. Heart disease and stroke statistics--2009 update: a report from the American Heart Association Statistics Committee and Stroke Statistics Subcommittee. *Circulation* 2009; 119:480-6.
2. Miller YI, Choi SH, Wiesner P, et al. Oxidation-specific epitopes are danger-associated molecular patterns recognized by pattern recognition receptors of innate immunity. *Circ Res* 2011; 108:235-48.
3. Lee S, Birukov KG, Romanoski CE, Springstead JR, Lusis AJ, Berliner JA. Role of phospholipid oxidation products in atherosclerosis. *Circ Res* 2012; 111:778-99.
4. Binder CJ, Shaw PX, Chang MK, et al. The role of natural antibodies in atherogenesis. *J Lipid Res* 2005; 46:1353-63.
5. Gargalovic PS, Gharavi NM, Clark MJ, et al. The unfolded protein response is an important regulator of inflammatory genes in endothelial cells. *Arterioscler Thromb Vasc Biol* 2006; 26:2490-6.
6. Gora S, Maouche S, Atout R, et al. Phospholipolyzed LDL induces an inflammatory response in endothelial cells through endoplasmic reticulum stress signaling. *FASEB J* 2010; 24:3284-97.
7. Pires NM, Jukema JW, Daemen MJ, Quax PH. Drug-eluting stents studies in mice: do we need atherosclerosis to study restenosis? *Vascul Pharmacol* 2006; 44:257-64.
8. Horkko S, Bird DA, Miller E, et al. Monoclonal autoantibodies specific for oxidized phospholipids or oxidized phospholipid-protein adducts inhibit macrophage uptake of oxidized low-density lipoproteins. *J Clin Invest* 1999; 103:117-28.
9. Marleau S, Harb D, Bujold K, et al. EP 80317, a ligand of the CD36 scavenger receptor, protects apolipoprotein E-deficient mice from developing atherosclerotic lesions. *FASEB J* 2005; 19:1869-71.
10. Binder CJ, Horkko S, Dewan A, et al. Pneumococcal vaccination decreases atherosclerotic lesion formation: molecular mimicry between *Streptococcus pneumoniae* and oxidized LDL. *Nat Med* 2003; 9:736-43.
11. Caligiuri G, Khallou-Laschet J, Vandaele M, et al. Phosphorylcholine-targeting immunization reduces atherosclerosis. *J Am Coll Cardiol* 2007; 50:540-6.
12. Faria-Neto JR, Chyu KY, Li X, et al. Passive immunization with monoclonal IgM antibodies against phosphorylcholine reduces accelerated vein graft atherosclerosis in apolipoprotein E-null mice. *Atherosclerosis* 2006; 189:83-90.
13. de FU, Su J, Hua X, et al. Low levels of IgM antibodies to phosphorylcholine predict cardiovascular disease in 60-year old men: Effects on uptake of oxidized LDL in macrophages as a potential mechanism. *J Autoimmun* 2009.
14. Gronlund H, Hallmans G, Jansson JH, et al. Low levels of IgM antibodies against phosphorylcholine predict development of acute myocardial infarction in a population-based cohort from northern Sweden. *Eur J Cardiovasc Prev Rehabil* 2009; 16:382-6.
15. Sjoberg BG, Su J, Dahlbom I, et al. Low levels of IgM antibodies against phosphorylcholine-A potential risk marker for ischemic stroke in men. *Atherosclerosis* 2009; 203:528-32.
16. Caidahl K, Hartford M, Karlsson T, et al. IgM-phosphorylcholine autoantibodies and outcome in acute coronary syndromes. *Int J Cardiol* 2012.
17. Ridker PM, Cannon CP, Morrow D, et al. C-reactive protein levels and outcomes after statin therapy. *N Engl J Med* 2005; 352:20-8.
18. Chang MK, Binder CJ, Miller YI, et al. Apoptotic cells with oxidation-specific epitopes are immunogenic and proinflammatory. *J Exp Med* 2004; 200:1359-70.
19. Chou MY, Fogelstrand L, Hartvigsen K, et al. Oxidation-specific epitopes are dominant targets of innate natural antibodies in mice and humans. *J Clin Invest* 2009; 119:1335-49.
20. Sampi M, Veneskoski M, Ukkola O, Kesaniemi YA, Horkko S. High plasma immunoglobulin (Ig) A and low IgG antibody titers to oxidized low-density lipoprotein are associated with markers of glucose metabolism. *J Clin Endocrinol Metab* 2010; 95:2467-75.
21. Su J, Georgiades A, Wu R, Thulin T, de FU, Frostegard J. Antibodies of IgM subclass to phosphorylcholine and oxidized LDL are protective factors for atherosclerosis in patients with hypertension. *Atherosclerosis* 2006; 188:160-6.
22. Gearhart PJ, Johnson ND, Douglas R, Hood L. IgG antibodies to phosphorylcholine exhibit more diversity than their IgM counterparts. *Nature* 1981; 291:29-34.
23. Briles DE, Forman C, Hudak S, Clafin JL. Anti-phosphorylcholine antibodies of the T15 idiotype

24. are optimally protective against *Streptococcus pneumoniae*. *J Exp Med* 1982; 156:1177-85.
24. Szu SC, Clarke S, Robbins JB. Protection against pneumococcal infection in mice conferred by phosphocholine-binding antibodies: specificity of the phosphocholine binding and relation to several types. *Infect Immun* 1983; 39:993-9.
25. Ewing MM, de Vries MR, Nordzell M, et al. Annexin A5 therapy attenuates vascular inflammation and remodeling and improves endothelial function in mice. *Arterioscler Thromb Vasc Biol* 2011; 31:95-101.
26. Lardenoye JH, Delsing DJ, de Vries MR, et al. Accelerated atherosclerosis by placement of a perivascular cuff and a cholesterol-rich diet in ApoE*3Leiden transgenic mice. *Circ Res* 2000; 87:248-53.
27. Hoet RM, Cohen EH, Kent RB, et al. Generation of high-affinity human antibodies by combining donor-derived and synthetic complementarity-determining-region diversity. *Nat Biotechnol*. 2005;23:344-8.
28. Beck A, Wurch T, Bailly C, Corvaia N. Strategies and challenges for the next generation of therapeutic antibodies. *Nat Rev Immunol* 2010; 10:345-52.
29. Tabas I. The role of endoplasmic reticulum stress in the progression of atherosclerosis. *Circ Res* 2010; 107:839-50.
30. Tabas I. Macrophage death and defective inflammation resolution in atherosclerosis. *Nat Rev Immunol* 2010; 10:36-46.
31. Hoogenboom HR. Selecting and screening recombinant antibody libraries. *Nat Biotechnol* 2005; 23:1105-16.
32. Lonberg N. Fully human antibodies from transgenic mouse and phage display platforms. *Curr Opin Immunol* 2008; 20:450-9.

Supplemental material

Methods

Cell cultures

Peripheral blood mononuclear cells (PBMCs) were isolated from citrated human blood using Ficoll-Paque PLUS (GE Healthcare) according to the instructions of the manufacturer. Monocytes were resuspended in serum free RPMI 1640 medium at density of 8×10^5 cells/ml and 250 μ L cell suspension was added into wells of a 96-well plate (2×10^5 cells/well). PBMC cells were treated with 2 μ g/mL Ox-LDL (Kalen Biomedical) in the presence or absence of up to 40 nM anti-PC IgG for 40 hours at 37°C, 5% CO₂.

Preparation and characterization of chimeric anti-PC T15 IgG

Anti-PC T15-IgG was constructed by synthesizing the DNA encoding the mouse variable regions and cloning the heavy and light chains into two different IgG expression vectors. To generate an IgG1 chimera the variable regions were cloned into an IgG1 expression vector, pRH1-f-CHO¹, such that the final antibody contains a fully human IgG1 Fc fragment consisting of human CH1, CH2, and CH3 with a mouse variable region. The heavy chain was cloned using the restriction enzymes BstXI and NheI and the light chain is cloned using the restriction enzymes ApalI and AsclI. The resulting T15-IgGs are mouse/human chimeras that contains mouse heavy and light variable regions and a human Fc region. The T15-IgG1 antibody was transiently expressed in 293T (human kidney) cells using FugeneHD (Roche) as the transfection reagent using Corning® CellStack® chambers (6360 cm² cell growth area). After 10 days of expression, the supernatant was harvested and antibody was initially purified using protein A sepharose (MabSelect, GE Healthcare) in which approximately 2.5 L of clarified cell culture media was applied (2 mL/min) over a 4.2 mL column equilibrated in PBS, washed with PBS containing an additional 0.4 M NaCl, and eluted with 50 mM Sodium Citrate, pH: 3.2. The pH of the eluted protein was adjusted to 5.0 and applied to a Poros HS (Applied Biosystems) ion exchange column (4.0 mL bed volume) at 2 mL/min equilibrated in 50 mM NaAcetate, pH: 5.0 and eluted with a linear gradient over 10 column volumes to 50 mM NaAcetate, 0.5 M NaCl, pH: 5.0. Eluted antibodies were buffer exchanged into Antibody Formulation Buffer (0.1 M citrate-phosphate, 50 mM NaCl, 0.01% Tween-80, 2% Trehalose, pH 6.0). Antibody concentrations were determined on purified samples by absorbance at 280 nm (1 mg/mL = 1.4 O.D.).

Mice

All animal experiments were approved by the Institutional Committee for Animal Welfare of the Leiden University Medical Center (LUMC). Transgenic male C57BL/6 ApoE*3-Leiden mice (bred in our own laboratory), aged 10-12 weeks at the start of a dietary run-in period, were used for this experiment.

Diets

Animals were fed a cholesterol-rich high-fat diet to induce hypercholesterolemia

containing 0.05% cholate (to improve intestinal cholesterol uptake and suppress bile acid synthesis, both leading to increased plasma cholesterol levels) and 1% cholesterol (as well as 20% casein, 1% choline chloride, 0.2% methionine, 15% cocoa butter, 40.5% sucrose, 10% cornstarch, 1% corn oil, 5.1% cellulose and 5.1% mineral mixture) (AB Diets). They received the diet three weeks prior to surgery and the diet was continued throughout the entire experiment. All animals received food and water ad libitum during the entire experiment.

Route of administration and treatment protocol

For all experiments, mice received intraperitoneal injections with antibody solutions (Dyax Corporation) in a volume of 100 μ l, using 100 μ l sterile 0.9% w/v NaCl (vehicle) as control, injected at the time of surgery (3 days) or twice weekly (14 days).

Vascular injury and accelerated atherosclerosis model²

After three weeks of diet, mice were anesthetized before surgery with a combination of Midazolam (5 mg/kg, Roche), Medetomidine (0.5 mg/kg, Orion) and Fentanyl (0.05 mg/kg, Janssen) through intraperitoneal injection. The right femoral artery was isolated and sheathed with a rigid non-constrictive polyethylene cuff (Portex) with 0.40 mm inner diameter, 0.80 mm outer diameter and an approximate length of 2.0 mm). Mice were sacrificed 3 or 14 days after cuff placement. For this, mice were anesthetized as before and euthanized.

The thorax was opened and mild pressure-perfusion (100mm Hg) with 3.7% formaldehyde in water (w/v) was performed for 5min by cardiac puncture in the left ventricle. After perfusion, the cuffed femoral artery was harvested, fixed overnight in 3.7% formaldehyde in water (w/v) and paraffin-embedded. Serial cross-sections (5 μ m thick) were taken from the entire length of the artery for histological analysis.

Immunoassays

After three weeks of diet (one day before surgery) and at the time of euthanasia, EDTA plasma samples were taken from the tail vein to determine total plasma cholesterol. Total plasma cholesterol (Boehringer Mannheim GmbH, kit 236691) concentration was measured enzymatically. Before surgery, mice were randomized in groups based on their total plasma cholesterol level. Enzyme-linked immuno sorbent assays (ELISA) were used to determine antibody titers. MCP-1 in cell supernatant was detected using the MCP-1 ELISA kit (R&D Systems), according to the manufacturer's instructions.

Vascular lesion quantification

The number of leukocytes, macrophages and cells expressing MCP-1, GRP78 BiP and CHOP attached to the endothelium or in the media of the femoral arteries was quantified and is displayed as a percentage of the total number of present cells. All quantification in this study was performed on six equally spaced (150 μ m distance) serial stained perpendicular cross-sections throughout the entire length of the vessel and was performed by blinded observers. Using image analysis software (Leica Qwin), the area containing SMCs and macrophages grafts was quantified morphometrically and is expressed as a percentage of the total cross-sectional vessel wall layer area. Additionally, total cross-sectional medial area was measured between

the external and internal elastic lamina and total cross-sectional intimal area was measured between the lumen and the internal elastic lamina.

Immunohistochemical stainings

Murine samples

All samples were stained with hematoxylin-phloxine-saffron (HPS). Weigert's elastin stain was used to visualize elastic laminae. Vessel wall sections undergoing immunological staining were pre-treated with a peroxidase block to decrease background staining due to endogenous peroxidase and with a concentrated solution of bovine serum albumin to block the adsorption of other proteins to non-specific binding sites on the vessel wall. Afterwards the primary antibody was added to the sections, left overnight and washed before the second antibody, specific to the primary antibody, was applied. After rinsing, an Avidin-Biotinylated enzyme complex was added to increase the sensitivity of the later to be added peroxidase Nova Red substrate, used as chromogen for colour development. Leukocytes were detected with the use of anti-CD45 antibodies (dilution 1:200, Pharmingen). Smooth muscle cells were stained with the use of anti-smooth muscle α -actin antibodies (dilution 1:800, Dako) and macrophages were detected with MAC3 staining (dilution 1:200, Pharmingen). MCP-1 expression was determined with the use of anti-mouse MCP-1 antibodies (dilution 1:300, Santa Cruz Biotechnology). The presence of ER stress and UPR was evaluated with antibodies against GRP78 BiP (GRP78 BiP, dilution 1:200, Abcam) and against CHOP (GADD153, dilution 1:200, Abcam).

Human aortic samples

The Tissue MicroArrays (TMA) included 20 aortic samples with atherosclerotic plaques from different individuals. The classification of the lesions was performed according to Stary³. For each lesion three representative areas were selected from hematoxylin- and eosin-stained sections of a donor block. Core cylinders (diameter: 0.6 mm) were punched and deposited into a recipient paraffin block using a specific arraying device (Beecher Instruments, Alphelys ring, MD)⁴. 5 μ m TMA sections were used for IHC analyses using digital slides (magnification 40) of each TMA spot which were acquired using Aperio ScanScope CS-US.

IHC was performed by using standard protocols with the following commercial primary antibodies directed against: CD68 (Dako; 1:500), alpha AML (Dako; 1:500), CD34 (Dako; 1:100), GRP78 (Abcam; 1:100) and ATF3 (Santa Cruz Biotechnology; 1:200) and noncommercial primary antibodies T15 (1:500) and M99 (1:50000). Briefly, IHC was performed on 5- μ m sections of TMA blocks. Deparaffinized and rehydrated sections were incubated for 30 min at room temperature with primary antibodies, washed, and incubated for 30 minutes with a Multilink kit (Biosys) for polyclonal antibodies and ABC Vector kit (Biosys) for monoclonal antibodies. After washing, the alkaline phosphatase/anti-alkaline phosphatase complexes and Fast Red TR substrate (Dako) or Ultravision LP detection System HRP DAB (MICROM) were added. Slides were counterstained with aqueous hematoxylin and mounted with Immunomount (Shandon).

Phage display selections

Phage display selections were performed using PC conjugated to bovine serum albumin (BSA) and to transferrin (Isosep AB) through a para-aminophenol linker using

isothiocyanate reaction chemistry. PC-BSA was produced at molar PC/BSA ratios of 1.4, 2.9, 5.7, and 22 mol PC/mol BSA. PC-transferrin was similarly prepared to contain 52 mol PC/mol transferrin. BSA was also reacted with just the para-aminophenol linker to serve as a reagent to remove antibody binders to the linker group from selected antibodies. PC modified BSA, PC modified transferrin, and linker modified BSA were biotinylated using EZ Link NHS-PEG4-Biotin (Pierce) to give molar incorporation ratios between 2 and 8 mol biotin per mol protein. Free biotinylation reagent was removed by dialysis against phosphate buffered saline (137 mM NaCl, 2.7 mM KCl, 4.3 mM Na₂HPO₄, 1.47 mM KH₂PO₄, pH 7.4). Biotinylation incorporation was determined using the 2-(4'-hydroxyazobenzene) benzoic acid (HABA) method according to the manufacturer (Pierce).

Phage display selections were performed using previously described antibody phage display procedures⁴ and antibody phage display libraries that combine natural and synthetic diversity⁵. Selections were initiated by first depleting the library of antibody binders to BSA, transferrin or the linker by incubating the library with the biotinylated depletion proteins immobilized on streptavidin coated magnetic beads (Invitrogen). The supernatant from the depletion step was then titered and incubated with biotinylated PC-protein conjugates that were immobilized on streptavidin coated magnetic beads (input titer in first round $\sim 2 \times 10^{12}$ pfu). Selection strategies alternated between panning on biotinylated PC-BSA in one round with panning on biotinylated PC-transferrin in the next round. Alternative selection strategies involved selecting on the same biotinylated PC-modified protein in each round. Prior to exposing the amplified phage from each selection round the phage were depleted using the biotinylated carrier protein in the absence of PC. In the case of selections on PC-BSA, the phage particles were first depleted with biotinylated BSA that contained the para-aminophenol linker molecule used to couple PC to BSA. Phage outputs after between 2 to 4 rounds of selection were isolated as individual phage isolates and screened for PC binding by phage ELISA.

Individual phage isolates were picked as colonies, grown overnight and the supernatant used in an ELISA to detect binding to biotinylated PC-BSA or biotinylated PC-transferrin immobilized on streptavidin coated plates as previously described using HRP-labeled anti-M13 and TMB substrate². ELISA positive hits were identified as having a target signal over background ratio greater than 3, where the target signal is the absorbance observed with target PC-BSA and PC-transferrin and the background is the signal observed with linker-BSA or transferrin, respectively. A total of 10560 phage clones was screened by ELISA to yield 1511 ELISA positive hits, which were subsequently found by DNA sequencing (Applied Biosystems 3730) to consist of 54 different antibody sequences.

IgG reformatting, expression and purification

The 54 different anti-PC antibodies were converted by batch sub-cloning the Fab fragments displayed on gene III of M13 phage into the pBRH1-f vector for the transient expression of fully human IgG1 (f-allotype) in 293T cells as previously described⁴. A total of 49 out of the 54 unique anti-PC antibodies were successfully recovered after batch sub-cloning and DNA sequencing as full length IgG1 antibodies. The remaining 5 antibodies were not recovered by DNA sequencing and were not pursued further.

DNA for each of the 49 IgGs was prepared from *E. coli* (DH5 α) using plasmid purification kits (Qiagen) and transfected into human kidney 293T cells to transiently generate IgG after a 10 day media harvest in a T175 flask. Purified IgG was recovered after a single step protein A sepharose (MabSelect, GE Healthcare) for 41 IgGs; the remaining 8 antibodies were either poorly expressed or not well purified and were consequently not pursued further. The 41 IgGs purified by protein A sepharose chromatography were used for *in vitro* binding studies (SPR and ELISA analysis). The IgGs with superior *in vitro* binding properties were produced in larger quantities for testing in *in vivo* animal as well as *in vitro* cell culture experiments and purified using both protein A sepharose and ion exchange chromatography as described above for the T15-IgG.

SPR analysis

IgGs were screened for binding to PC using a surface plasmon resonance (SPR) biosensor (Biacore 3000). Aminophenylphosphorylcholine (Biosearch Technologies) was coupled through the free amine group to one flow cell of a CM5 chip to a density of 120 RU. To another flow cell of the same CM5 chip the counter screen reagent 4-aminophenyl phosphate (Gold Biotechnology) was amine coupled to a density of approximately 120 RU. PC-KLH (Biosearch Technologies) and PC-BSA were also coupled to separate flow cells of a CM5 chip. Using these surfaces with PC immobilized in different contexts, the antibodies were injected at 100 nM at 50 μ L/min and binding sensorgrams were obtained. Binding was assessed by recording the signal at the end of the injection.

Antibody binding assays

Oxidized LDL (5 μ g) was coated on the surface of a 384-well ELISA in PBS by overnight incubation at 4°C. The plate was blocked with 2% BSA and washed 5 times with PBST before 50 μ L of the antibody at different concentrations was added. Unbound antibody was removed by washing with PBST and bound antibody was detected using a 1:5000 dilution of HRP labeled goat anti-human IgG, Fc- γ specific secondary antibody with a TMB colorimetric substrate.

Apoptotic cell binding assays

Jurkat T cells (ATCC) were cultured in RPMI 1640 media supplemented with 10% FBS, penicillin (100 U/mL) and streptomycin (100 μ g/mL). Cells were harvested by centrifugation, washed with ice-cold PBS and aliquoted into wells of a 96-well plate. Cells were blocked with 5% BSA in PBS at 4°C for 30 minutes prior to incubation with anti-PC antibodies at a concentration of 20 μ g/mL in PBS containing 5% BSA at 4°C for an additional 30 minutes. A recombinant human IgG1 (A2) with a binding specificity towards streptavidin was used as an isotype control. After washing with PBS containing 5% BSA, cells were incubated with the secondary antibody (FITC-conjugated goat anti-human IgA, IgG, or IgM, Thermo) at a dilution of 1:50 in PBS containing 5% BSA. Prior to washing the cells, 5 μ L of APC- annexin V antibody (BD Biosciences) was added. After the cells were washed, they were resuspended cells in PBS with 5% BSA and 1 μ L of 1 mg/mL propidium iodide per sample. Cells were analyzed by flow cytometry using the LSRII instrument from BD Biosciences.

Construction of germline and stability mutants of anti-PC M99-B05 IgG

The amino acid sequence of the M99-B05 anti-PC IgG was inspected in order to identify potential amino acid substitutions that could reduce potential immunogenicity of the antibody in human and avoid susceptible amino acid modification that may occur during antibody expression and purification. Substitutions that could make the antibody less immunogenic were identified by aligning the amino acid sequence of M99-B05 with the most closely related germline antibody sequence from the Kabat database. The heavy chain of M99-B03 was compared to the VH3-23, JH3 heavy chain and the light chains were compared to the VK4-B3, JK1 light chain germline sequence. The variant X19-A05 incorporates a total of 9 mutations that include germline substitutions as well as substitution to remove potential deamidation sites. The X19-A05 was transiently expressed and purified as described above for antibodies to be tested in in vivo experiments.

Statistical analysis

All data are presented as mean \pm standard error of the mean (SEM), unless otherwise indicated. Overall comparisons between data from groups were performed using the Kruskal-Wallis test. If a significant difference was found, groups were compared using a Mann-Whitney sum test. All statistical analyses were performed with SPSS 16.0 software for Windows. P-values less than 0.05 were regarded as to be statistically significant and are indicated with an asterisk (*).

Reference List

1. Jostock T, Vanhove M, Brepoels E, et al. Rapid generation of functional human IgG antibodies derived from Fab-on-phage display libraries. *J Immunol Methods* 2004; 289:65-80.
2. Ewing MM, de Vries MR, Nordzell M, et al. Annexin A5 therapy attenuates vascular inflammation and remodeling and improves endothelial function in mice. *Arterioscler Thromb Vasc Biol* 2011; 31:95-101.
3. Stary, H. C., Chandler, B. A., Glagov, S., et al. A definition of initial, Fatty Streak, and Intermediate Lesion of Atherosclerosis. *Arterioscler Thromb* 1994;14:840-56.
4. Richter, J., Wagner, U., Kononen, J., et al. High-throughput tissue microarray analysis of cyclin E gene amplification and overexpression in urinary bladder cancer. *Am J Pathol* 2000;157:787-94.
5. Buckler DR, Park A, Viswanathan M, Hoet RM, Ladner RC. Screening isolates from antibody phage-display libraries. *Drug Discov Today* 2008; 13:318-24.
6. Hoet RM, Cohen EH, Kent RB, et al. Generation of high-affinity human antibodies by combining donor-derived and synthetic complementarity-determining-region diversity. *Nat Biotechnol* 2005; 23:344-8.

Supplemental figures

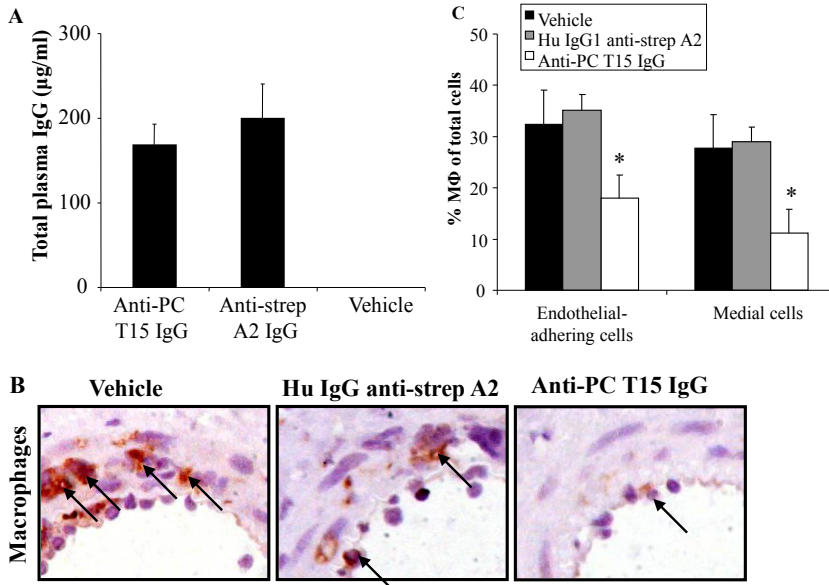


Figure I (A) Total plasma antibody IgG concentration (µg/ml) of ApoE3*Leiden mice receiving vehicle, human anti-streptavidin or anti-PC T15 IgG after 3d. (B) Representative cross-sections (MAC3 staining, magnification 80x). (C) Quantification of macrophages in the intima and media (% of all cells). Results indicated as mean±SEM, n=10. * p<0.05.

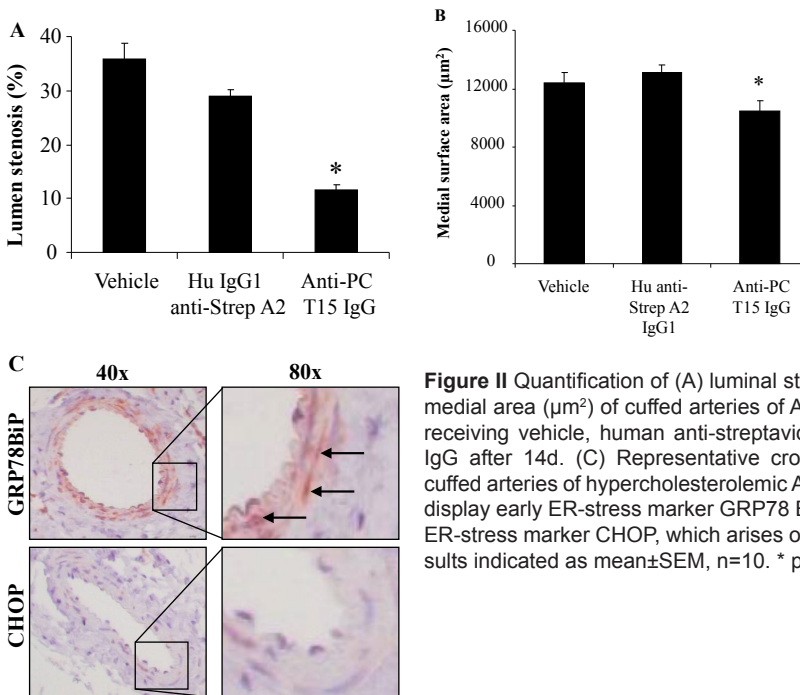


Figure II Quantification of (A) luminal stenosis (%) and (B) medial area (µm²) of cuffed arteries of ApoE3*Leiden mice receiving vehicle, human anti-streptavidin or anti-PC T15 IgG after 14d. (C) Representative cross-sections of uncuffed arteries of hypercholesterolemic ApoE3*Leiden mice display early ER-stress marker GRP78 BiP, but not the late ER-stress marker CHOP, which arises only after injury. Results indicated as mean±SEM, n=10. * p<0.05.

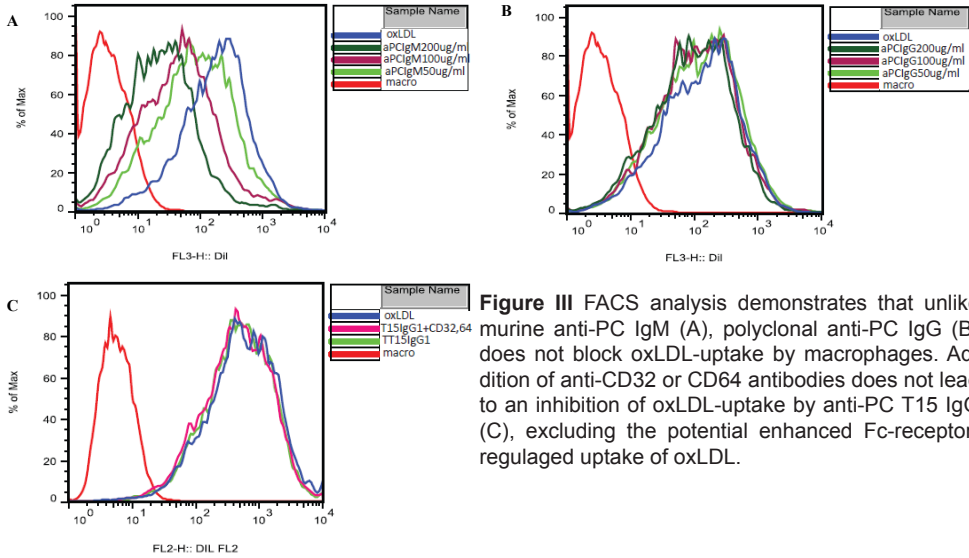
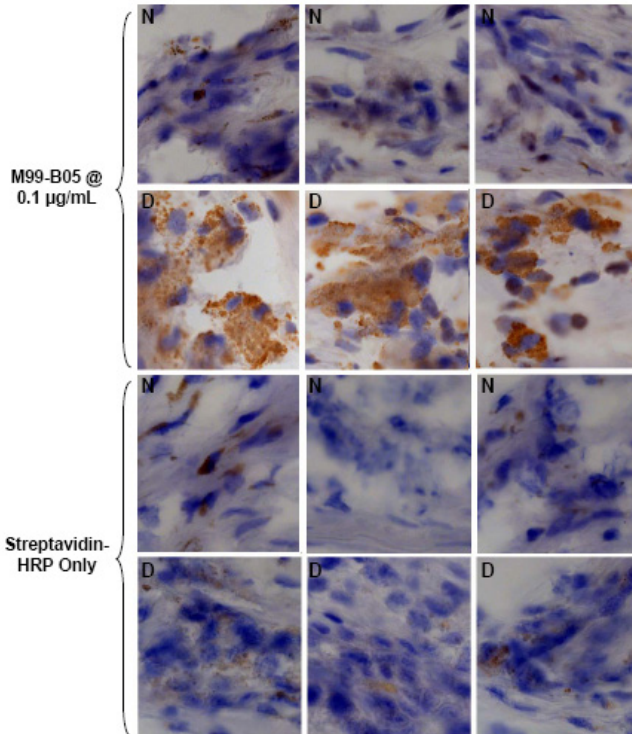


Figure III FACS analysis demonstrates that unlike murine anti-PC IgM (A), polyclonal anti-PC IgG (B) does not block oxLDL-uptake by macrophages. Addition of anti-CD32 or CD64 antibodies does not lead to an inhibition of oxLDL-uptake by anti-PC T15 IgG (C), excluding the potential enhanced Fc-receptor-regulated uptake of oxLDL.

A

Immunohistochemistry Staining of Phosphorylcholine in Human Non-Diseased and Atherosclerotic Aorta



N= Non-Diseased Aorta; D= Atherosclerotic Aorta

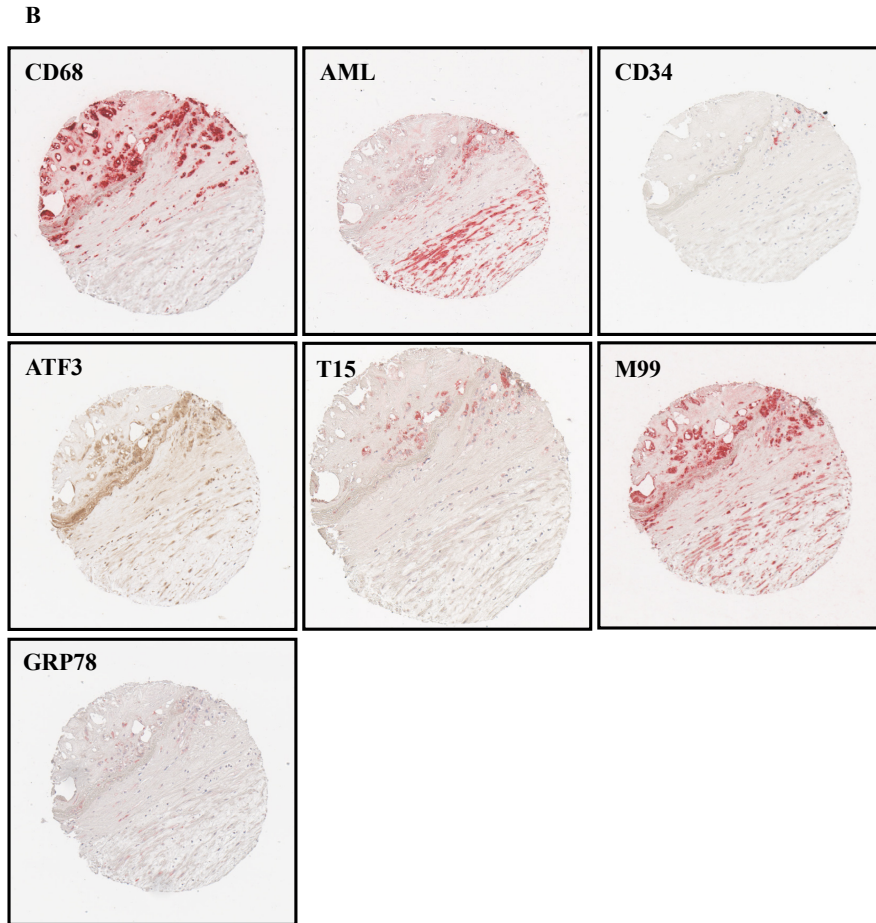


Figure IV Representative cross-sections of (A) human non-diseased and atherosclerotic aortic tissue (anti-PC M99B05 and HRP streptavidin staining, magnification 20x) and (B) IHC studies on the serial sections of TMA of human aortic fibroatheromatous plaques (original magnification 100x). The representative sections are shown: CD68 staining is specific for monocyte/macrophages and foam cells of monocyte origin, alpha AML staining is specific for smooth muscle cells and CD34 staining is specific for endothelial cell. T15 and M99 stainings correspond to PC.

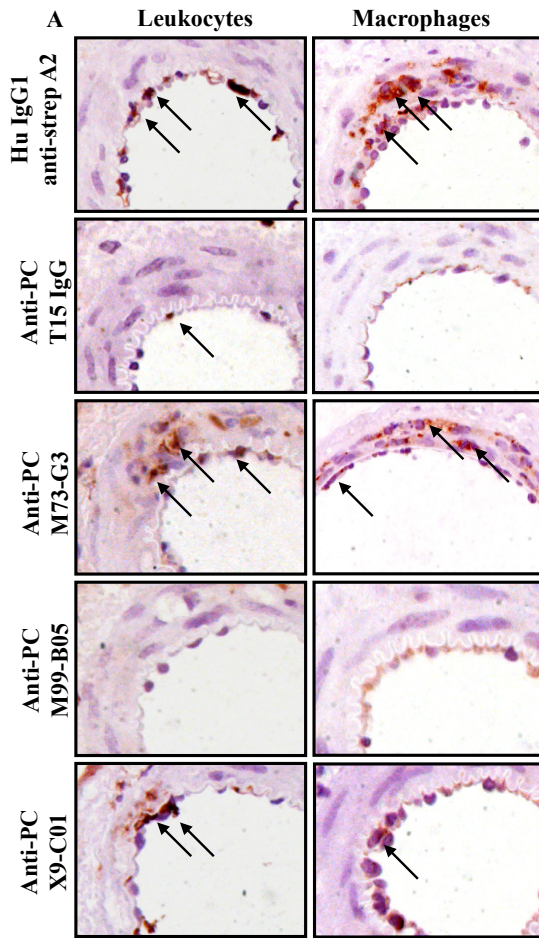


Figure V (A) Representative cross-sections of cuffed arteries of ApoE3*Leiden mice receiving human anti-streptavidin, anti-PC T15 IgG, anti-PC M73-G3, anti-PC M99-B05 or anti-PC X9-C01 after 3d (MAC3 and CD45 staining, magnification 40x, arrows indicate leukocytes and macrophages).

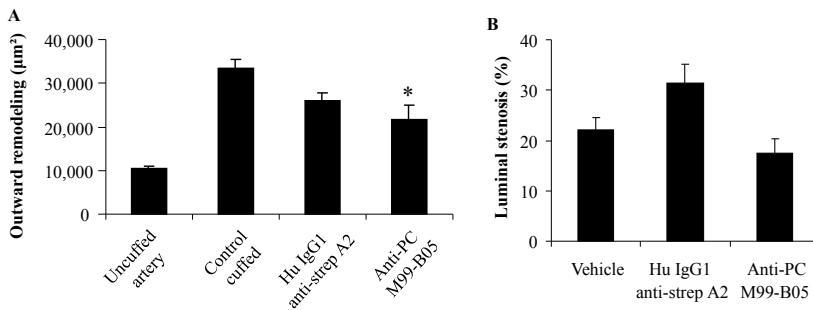
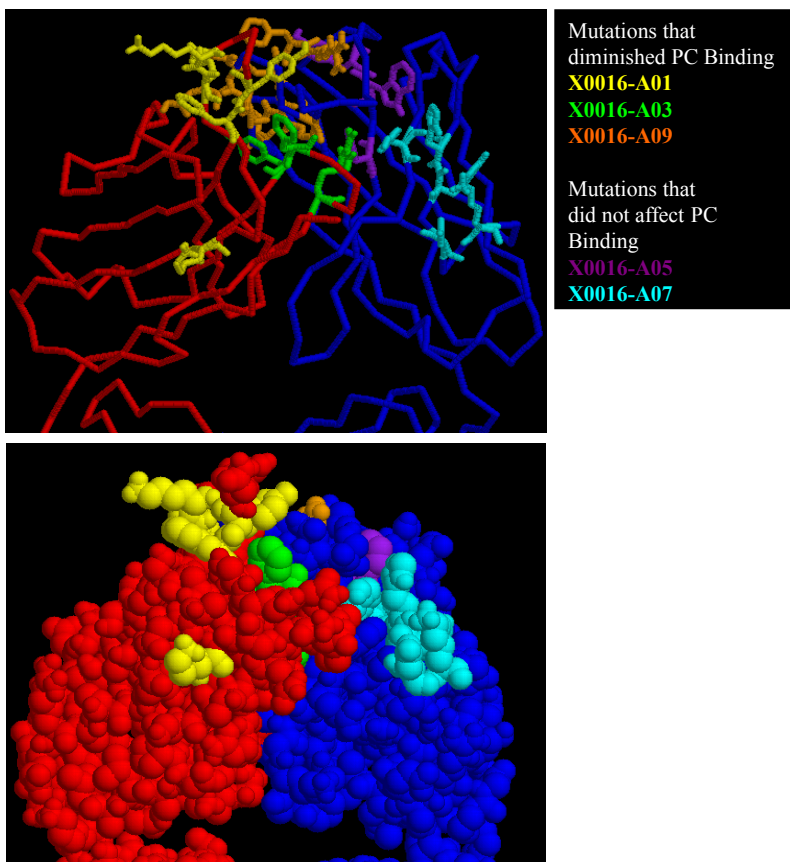


Figure VI Quantification of (A) outward remodeling (μm^2) and (B) lumen stenosis (%) of ApoE3*Leiden mice receiving vehicle, human anti-streptavidin or anti-PC M99-B05 after 14d. Results indicated as mean \pm SEM, n=10. * p<0.05.

A 3-D model of M99-B05**B****M99-B05 Heavy Chain Sequences**

M99-B05 EVQLLESGGGLVQPGGSLRLSCAASGFT-SGYWMHWVRQAPGKGLEWVSY
M99-B05 ISPSGGGTHYADSVKGRFTISRDNKNTLYQMNSLRAEDTAVYYCARVR
M99-B05 FRVCSNGVCRPTAYDAFDIWGQGTAVTVSS

C**M99-B05 Light Chain Sequences**

M99-B05 QDIQMTQSPDLSAVSLGERATINCKSSQSVFYNSNKKNYLAWYQQKAGQPP
M99-B05 KLLIHWASTRESGVPDRFSGSGSGTDFLTISNLAQEDVALYCCQQYFNA
M99-B05 PRTFGQGTKVEIK

Figure VII (A) A 3-D model of M99-B05 was constructed by grafting the antibody sequence onto existing structures of similar antibodies. From the above information on which mutations disrupted PC binding it was able to obtain approximations from the model on where the PC antigen may be binding. Analysis suggests that M99-B05 binds PC through an antibody structure that involves multiple CDRs at the interface between the light and heavy chains. The light chain is shown in red and the heavy chain is shown in blue. (B) Heavy chain sequence optimization of M99-B05. (C) Light chain sequence optimization of M99-B05.

Antibody stability in human serum

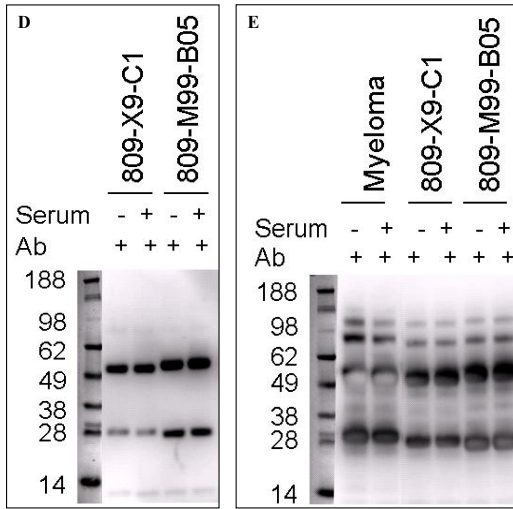


Figure VII Western blot analysis with HRP-conjugated goat anti-human IgG (D) or HRP-conjugated streptavidin (E). Both antibodies are stable in serum under the tested conditions, as evidenced by the lack of degradation in the band intensity of the heavy chain (band above the 49kDa marker) and the light chain (band near the 28 kDa marker). Ab Antibody.

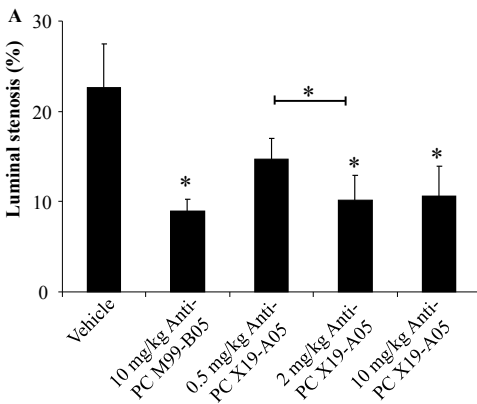


Figure VIII Quantification of (A) luminal stenosis (%) of ApoE3*Leiden mice receiving vehicle, 10mg/kg anti-PC M99-B05 or 0.5, 2 or 10mg/kg X19-A05 after 14d. Results indicated as mean±SEM, n=10. * p<0.05.

Quantification of arterial wall phenotype

| Group | Leukocyte area (%) | | Macrophage area (%) | | SMC area (%) | |
|-----------------------|--------------------|----------|---------------------|-----------|--------------|-----------|
| | Intima | Media | Intima | Media | Intima | Media |
| Vehicle | 22.3±2.7 | 25.4±4.5 | 44.3±5.9 | 54.9±6.1 | 34.0±4.2 | 33.1±4.1 |
| Hu IgG1 anti-strep A2 | 18.9±2.1 | 17.0±2.8 | 36.9±4.4 | 45.0±3.2 | 41.4±3.7 | 45.1±2.6 |
| Anti-PC T15 IgG | 7.5±1.2* | 6.5±1.8* | 11.3±2.0* | 15.3±3.1* | 35.8±3.9 | 61.8±3.8* |

Table I Quantification of arterial wall phenotype.

Quantification of leukocyte area (%), macrophage area (%) and SMC area (%) in the tunica intima and media of the cuffed femoral artery of ApoE3*Leiden mice receiving vehicle, human anti-streptavidin or anti-PC T15 IgG after 14d. Results indicated as mean±SEM, n=10. * p<0.05.

Total plasma cholesterol (mmol/L)

| Group | Surgery | Sacrifice |
|--------------------------------|----------|-----------|
| 10 mg/kg Anti-PC IgG | 13.3±2.5 | 18.7±1.4 |
| 10 mg/kg Hu IgG1 anti-strep A2 | 11.1±0.9 | 13.8±0.6 |
| Vehicle | 10.8±1.0 | 19.2±1.4 |
| 10 mg/kg Anti-PC M73-G3 | 9.9±2.0 | 12.4±2.4 |
| 10 mg/kg Anti-PC M99-B05 | 9.1±1.8 | 9.5±1.8 |
| 10 mg/kg Anti-PC X9-C01 | 9.0±1.5 | 12.5±2.2 |
| 10 mg/kg anti-PC T15 IgG | 8.3±1.4 | 10.6±1.8 |
| 10 mg/kg Hu IgG1 anti-strep A2 | 10.5±2.0 | 13.3±2.3 |
| Vehicle | 14.4±2.4 | 12.4±2.3 |
| 10 mg/kg Hu IgG1 anti-strep A2 | 12.5±1.6 | 11.4±2.4 |
| 10 mg/kg Anti-PC M99-B05 | 9.9±1.1 | 10.6±1.2 |
| 10 mg/kg Anti-PC X19-A05 | 11.0±1.0 | 9.9±1.0 |
| 2 mg/kg Anti-PC X19-A05 | 9.7±0.8 | 8.3±0.3 |
| 0.5 mg/kg Anti-PC X19-A05 | 10.4±0.8 | 10.5±0.5 |
| 10 mg/kg Anti-PC M99-B05 | 9.5±0.7 | 8.4±0.5 |
| 10 mg/kg Hu IgG1 anti-strep A2 | 11.2±1.0 | 10.8±2.2 |

Table 2 Plasma cholesterol concentrations.

Plasma total cholesterol (mmol/L) of ApoE3*Leiden mice receiving vehicle, human anti-streptavidin, anti-PC T15 IgG, anti-PC M73-G3, anti-PC M99-B05, anti-PC X9-C01 or X19-A05, measured at surgery or at sacrifice (day 3 or 14). Results indicated as mean±SEM, n=10. No statistical significant differences were observed.

Plasma antibody concentrations

| Group | Total IgG ($\mu\text{g/ml}$) | Anti-PC IgG ($\mu\text{g/ml}$) |
|--------------------------------|-----------------------------------|-------------------------------------|
| 10 mg/kg Anti-PC IgG | 169 \pm 76.0 | 1208 \pm 329 |
| 10 mg/kg Hu IgG1 anti-strep A2 | 200 \pm 131 | 0.8 \pm 0.3 |
| Vehicle | 0.4 \pm 0.1 | 0.5 \pm 0.1 |
| 10 mg/kg Anti-PC M73-G3 | 58.3 \pm 6.3 | n.d. |
| 10 mg/kg Anti-PC M99-B05 | 54.6 \pm 11.4 | n.d. |
| 10 mg/kg Anti-PC X9-C01 | 3.5 \pm 0.6 | n.d. |
| 10 mg/kg anti-PC T15 IgG | 103 \pm 25.6 | n.d. |
| 10 mg/kg Hu IgG1 anti-strep A2 | 70.9 \pm 14.0 | n.d. |
| Vehicle | 0.4 \pm 1.0 | 0.3 \pm 0.2 |
| 10 mg/kg Hu IgG1 anti-strep A2 | 142 \pm 76.4 | 0.2 \pm 0.0 |
| 10 mg/kg Anti-PC M99-B05 | 49.1 \pm 99.4 | 65.6 \pm 47.4 |
| 10 mg/kg Anti-PC X19-A05 | 42.2 \pm 23.8 | 9.9 \pm 1.0 |
| 2 mg/kg Anti-PC X19-A05 | 3.3 \pm 6.6 | 8.3 \pm 0.3 |
| 0.5 mg/kg Anti-PC X19-A05 | 2.9 \pm 2.5 | 10.5 \pm 0.5 |
| 10 mg/kg Anti-PC M99-B05 | 12.8 \pm 15.1 | 8.4 \pm 0.5 |
| 10 mg/kg Hu IgG1 anti-strep A2 | 155 \pm 33.5 | 10.8 \pm 2.2 |

Table 3 Plasma antibody titers.

Plasma total IgG ($\mu\text{g/ml}$) and anti-PC IgG ($\mu\text{g/ml}$) antibody concentration in ApoE3*Leiden mice receiving vehicle, human anti-streptavidin, anti-PC T15 IgG, anti-PC M73-G3, anti-PC M99-B05, anti-PC X9-C01 or X19-A05, measured at surgery or at sacrifice (day 3 or 14). Results indicated as mean \pm SEM, n=10. Between groups, no statistical significant differences were observed. n.d. not determined.

